Inorg. Chem. **2007**, *46*, 3903–3915

Synthesis and Characterization of Vanadium(IV) Complexes with *cis*-Inositol in Aqueous Solution and in the Solid-State†

Bernd Morgenstern,‡ Barbara Kutzky,‡ Christian Neis,‡ Stefan Stucky,‡ Kaspar Hegetschweiler,*,‡ Eugenio Garribba,*,§ and Giovanni Micera§

Anorganische Chemie, Universität des Saarlandes, Postfach 15 11 50, D-66041 Saarbrücken, Germany, and Dipartimento di Chimica, Universitá degli Studi di Sassari, Via Vienna 2, I-07100 Sassari, Italy

Received September 27, 2006

The complex formation of vanadium(IV) with *cis*-inositol (ino) and the corresponding trimethyl ether 1,3,5-trideoxy-1,3,5-trimethoxy-*cis*-inositol (tmci) was studied in aqueous solution and in the solid-state. With increasing pH, the formation of $[VO(H_{-2}L)]$, $[(VO)_2L_2H_{-5}]^-$, $[VO(H_{-3}L)]^-$ (L = ino) or $[(VO)_2L_2H_{-6}]^{2-}$ (L = tmci), $[V(H_{-3}L)_2]^{2-}$, and $[VO(H_{-3}L)(OH)_2]^{3-}$ was observed. For the vanadium(IV)/ino system, $[(VO)_2L_2H_{-7}]^{3-}$ was observed as an additional dinuclear species. The formation constants of these complexes were determined by potentiometric titrations (25 °C, 0.1 M KCl). In addition, the vanadium(IV)/ino system was investigated by means of UV–vis spectrophotometric methods. EPR spectroscopy and cyclic voltammetry confirmed this complexation scheme. EPR measurements indicated the formation of three distinct isomers of the non-oxo complex $[V(H_{-3}ino)_2]^{2-}$ in weakly basic solution. This type of isomerism, which is not observed for the vanadium(IV)/tmci system, was assigned to the ability of ino to bind the vanadium(IV) center with three alkoxo groups having either a 1,3,5-triaxial or an 1,2,3-axial–equatorial–axial arrangement. The structures of $[V(H_{-3}ino)_2][K_2(ino)_2]\cdot 4H_2O$ (**1**) and $[Na_6V(H_{-3}ino)_2](SO_4)_2\cdot 6H_2O$ (**2**) were determined by single-crystal X-ray analysis. In both compounds, the coordination of each ino molecule to the vanadium(IV) center via three axial deprotonated oxygen donors was confirmed. The centrosymmetric structure of the coordination spheres corresponds to an almost regular octahedral geometry with a twist angle of 60°. The crystal structure of the potassium complex **1** represents an unusual 1:1 packing of $[V(H_{-3}ino)_2]^{2-}$ dianions and $[K_2(ino)_2]^{2+}$ dications, in which both K^+ ions have a coordination number of nine and are bonded simultaneously to a 1,3,5-triaxial and an 1,2,3-axial–equatorial–axial site of ino. In **2**, the $[V(H_{-3}ino)_2]^{2-}$ complexes are surrounded by six Na^+ counterions that are bonded to the axial alkoxo oxygens and to the equatorial hydroxy oxygens of the *cis*-inositolato moieties. The six Na^+ centers are further interlinked by bridging sulfate ions. According to EPR spectroscopy, the D_{3d} symmetric structure of the $[V(H_{-3}ino)_2]^{2-}$ anion is retained in H_2O, in dimethylformamide, and in a mixture of $CHCl_3$/toluene 60:40 v/v.

Introduction

Vanadium is an important trace element for different organisms.[1,2] Among others, it is present in vanadium-dependent haloperoxidases,[3] in nitrogenases,[4,5] and is accumulated in concentrations of up to 0.3 M in the vanadocytes of various sea squirts.[6] In 1980 and more recently,

† Metal Binding of Polyalcohols. 8. Part 7: Sander, J.; Hegetschweiler, K.; Morgenstern, B.; Keller, A.; Amrein, W.; Weyhermüller, T.; Müller, I. *Angew. Chem. Int. Ed.* **2001**, *40*, 4180−4182.

* Corresponding author. E-mail: hegetschweiler@mx.uni-saarland.de (K.H.); garribba@uniss.it (E.G.).

‡ Universität des Saarlandes.

§ Universitá degli Studi di Sassari.

(1) Rehder, D. In *Metal Ions in Biological Systems*; Sigel, A.; Sigel, H., Eds.; Marcel Dekker: New York, 1995; Vol. 31, pp 1−43.

(2) Crans, D. C.; Smee, J. J.; Gaidamauskas, E.; Yang, L. *Chem. Rev.* **2004**, *104*, 849−902 and references therein.

(3) Pecoraro, V. L.; Slebodnick, C. A.; Hamstra, B. J. In *Vanadium Compounds: Chemistry, Biochemistry, and Therapeutic Applications*; Tracey, A. S.; Crans, D. C. Eds.; ACS Symposium Series 711, Washington, DC, 1998; pp 157−167.

(4) Robson, R. L.; Eady, R. R.; Richardson, T. H.; Miller, R. W.; Hawkins, M.; Postgate, J. R. *Nature* **1986**, *322*, 388−390.

(5) Eady, R. R. In *Metal Ions in Biological Systems*; Sigel, A.; Sigel, H., Eds.; Marcel Dekker: New York, 1995; Vol. 31, pp 363−405 and references therein.

(6) Smith, M. J.; Ryan, D. E.; Nakanishi, K.; Frank, P.; Hodgson, K. O. In *Metal Ions in Biological Systems*; Sigel, A.; Sigel, H., Eds.; Marcel Dekker: New York, 1995; Vol. 31, pp 423−490.

10.1021/ic0618504 CCC: $37.00
Published on Web 04/10/2007

it has been demonstrated that many vanadium compounds have therapeutic effects as insulin-enhancing agents.[7−9]

The chemistry of vanadium(IV) is dominated by the vanadyl ion, VO^{2+}, one of the most stable diatomic cations. However, non-oxo vanadium centers hold important biological functions and have also been reported for (i) amavadin, a complex isolated by Bayer and Kneifel from Amanita muscaria[10] and characterized by Carrondo et al.[11] and Garner and co-workers [12] and (ii) the cofactor of vanadium nitrogenase.[4,5] This has stimulated the synthesis and investigation of new non-oxo species in the last 10 years.[13] However, the number of such non-oxo complexes found within the electronic Cambridge Structural Database still remains relatively low.[14] This is due mainly to the stability of the vanadium−oxygen double bond, which renders the synthesis of octahedrally coordinated vanadium(IV) non-oxo species rather difficult.

In a recent paper,[15] we demonstrated that 1,3,5-triamino-1,3,5-trideoxy-*cis*-inositol (taci)[16−19] and 1,3,5-trideoxy-1,3,5-tris(dimethylamino)-*cis*-inositol (tdci)[20] are able to form bischelated non-oxo vanadium(IV) species with a D_{3d} symmetric VO_6 coordination. Unlike other complexing agents such as the catecholates,[21] a stoichiometric amount of these ligands was sufficient to generate quantitatively mononuclear non-oxo species in neutral and alkaline solutions. In contrast to the polyamino−polyalcohol taci, which offers four different coordination modes for metal binding, the pure polyalcohol *cis*-inositol (ino) can bind a metal center only in two different ways, either via a 1,3,5-triaxial (ax−ax−ax) or an 1,2,3-axial−equatorial−axial (ax−eq−ax) coordination mode (Scheme 1a). The adoption of a particular mode depends on the size of the cation; metal ions with an ionic radius smaller than 0.8 Å are preferentially bound to the (ax−ax−ax) and larger ions are preferentially bound to the (ax−eq−ax) site.[22] One would thus expect that a hexa-coordinated V^{4+} ion with a radius of 0.58 Å adopts an (ax−ax−ax) structure.[23] However, the transformation to an (ax−eq−ax) coordination would require a relatively low amount of energy. Such considerations have been verified for Fe^{3+} (ionic radius = 0.65 Å), where both modes have been observed in the solid-state structure of $[OFe_6(ino)_6H_{-21}]^{5-}$.[24]

Scheme 1. Coordination Modes of ino and tmci

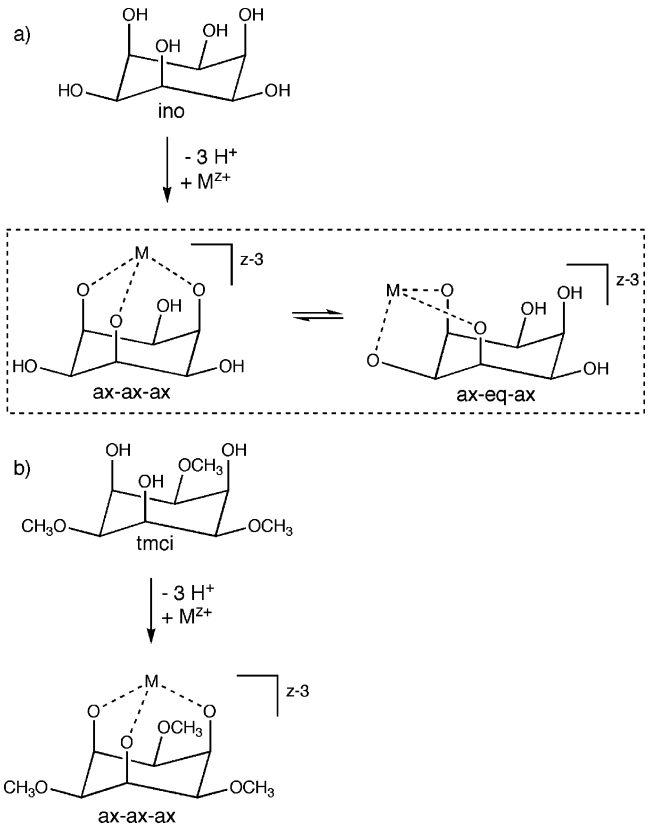

To shed light on the possibility of forming such different vanadium(IV)/ino species, we prepared 1,3,5-trideoxy-1,3,5-trimethoxy-*cis*-inositol (tmci) as a new facially-coordinating triol ligand, which is presented here for the first time (Scheme 1b). In contrast to ino, the binding properties of this trimethylether are restricted to an (ax−ax−ax) mode, provided that the generation of negative oxygen donors is a

(7) Shechter, Y.; Karlish, S. J. D. *Nature* **1980**, *284*, 556−558.
(8) Thompson, K. H.; McNeill, J. H.; Orvig, C. *Chem. Rev.* **1999**, *99*, 2561−2571 and references therein.
(9) Shechter, Y.; Goldwaser, I.; Mironchik, M.; Fridkin, M.; Gefel, D. *Coord. Chem. Rev.* **2003**, *237*, 3−11.
(10) (a) Bayer, E.; Kneifel, H. *Z. Naturforsch. B* **1972**, *27*, 207−207. (b) Kneifel, H.; Bayer, E. *Angew. Chem. Int. Ed. Engl.* **1973**, *12*, 508−509.
(11) (a) Carrondo, M. A. A. F. de C. T.; Duarte, M. T. L. S.; Costa Pessoa, J.; Silva, J. A. L.; Fraústo da Silva, J. J. R.; Vaz, M. C. T. A.; Vilas-Boas, L. F. *J. Chem. Soc. Chem. Commun.* **1988**, 1158−1159. (b) Carrondo, M. A. A. F. de C. T.; Duarte, M. T. L. S.; Fraústo da Silva, J. J. R.; da Silva, J. A. L. *Struct. Chem.* **1992**, *3*, 113−119.
(12) (a) Smith, P. D.; Berry, R. E.; Harben, S. M.; Beddoes, R. L.; Helliwell, M.; Collison, D.; Garner, C. D. *J. Chem. Soc. Dalton Trans*. **1997**, 4509−4516. (b) Berry, R. E.; Armstrong, E. M.; Beddoes, R. L.; Collison, D.; Ertok, S. N.; Helliwell, M.; Garner, C. D. *Angew. Chem. Int. Ed*. **1999**, *38*, 795−797.
(13) (a) Vergopoulos, V.; Jantzen, S.; Rodewald, D.; Rehder D. *J. Chem. Soc. Chem. Commun.* **1995**, 377−378. (b) Ludwig, E.; Hefele, H.; Uhlemann, E.; Weller, F.; Kläui, W. *Z. Anorg. Allg. Chem.* **1995**, *621*, 23−28. (c) Hefele, H.; Ludwig, E.; Uhlemann, E.; Weller, F. *Z. Anorg. Allg. Chem*. **1995**, *621*, 1973−1976. (d) Klich, P. R.; Daniher, A. T.; Challen, P. R.; McConville, D. B.; Youngs, W. J. *Inorg. Chem.* **1996**, *35*, 347−356. (e) Kondo, M.; Minakoshi, S.; Iwata, K.; Shimizu, T.; Matsuzaka, H.; Kamigata, N.; Kitagawa, S. *Chem. Lett.* **1996**, 489−490. (f) Kang, B. S.; Wang, X. J.; Su, C. Y.; Liu, H. Q.; Wen, T. B.; Liu, Q. T. *Transition Met. Chem.* **1999**, *24*, 712−717. (g) Paine, T. K.; Weyhermüller, T.; Bill, E.; Bothe, E.; Chaudhuri, P. *Eur. J. Inorg. Chem.* **2003**, 4299−4307. (h) Paine, T. K.; Weyhermüller, T.; Slep, L. D.; Neese, F. Bill, E.; Bothe, E.; Wieghardt, K.; Chaudhuri, P. *Inorg. Chem*. **2004**, *43*, 7324−7338.
(14) Allen, F. H.; Kennard, O. *Chem. Des. Autom. News* **1993**, *8*, 31−37.
(15) Morgenstern, B.; Steinhauser, S.; Hegetschweiler, K.; Garribba, E.; Micera, G.; Sanna, D.; Nagy, L. *Inorg. Chem*. **2004**, *43*, 3116−3126.
(16) Hegetschweiler, K. *Chem. Soc. Rev.* **1999**, *28*, 239−249.
(17) Hegetschweiler, K.; Gramlich, V.; Ghisletta, M.; Samaras, H. *Inorg. Chem*. **1992**, *31*, 2341−2346.
(18) Ghisletta, M.; Hausherr-Primo, L.; Gajda-Schrantz, K.; Machula, G.; Nagy, L.; Schmalle, H. W.; Rihs, G.; Endres, F.; Hegetschweiler, K. *Inorg. Chem*. **1998**, *37*, 997−1008.
(19) Hegetschweiler, K.; Ghisletta, M.; Fässler, T. F.; Nesper, R.; Schmalle, H. W.; Rihs, G. *Inorg. Chem*. **1993**, *32*, 2032−2041.
(20) (a) Hegetschweiler, K.; Kradolfer, T.; Gramlich, V.; Hancock, R. D. *Chem. −Eur. J*. **1995**, *1*, 74−88. (b) Hegetschweiler, K.; Raber, T.; Reiss, G. J.; Frank, W.; Wörle, M.; Currao, A.; Nesper, R.; Kradolfer, T. *Angew. Chem., Int. Ed. Engl.* **1997**, *36*, 1964−1966.
(21) Branca, M.; Micera, G.; Dessí, A.; Sanna, D.; Raymond, K. N. *Inorg. Chem*. **1990**, *29*, 1586−1589.
(22) Hancock, R. D.; Hegetschweiler, K. *J. Chem. Soc. Dalton Trans*. **1993**, 2137−2140.
(23) Shannon, R. D. *Acta. Crystallogr*. **1976**, *A32*, 751−767.
(24) Hegetschweiler, K.; Hausherr-Primo, L.; Koppenol, W. H.; Gramlich, V.; Odier, L.; Meyer, W.; Winkler, H.; Trautwein, A. X. *Angew. Chem., Int. Ed. Engl*. **1995**, *34*, 2242−2243.

prerequisite for the vanadium(IV) coordination. In this work, potentiometric, spectroscopic, electrochemical, and structural data of the vanadium(IV)/ino system will be presented, and the relevant differences between the coordinating properties of ino and tmci will be discussed.

Experimental Section

Materials, Instrumentation, and Analyses. Ino was prepared as described previously.[25] Other chemicals were commercially available and were used as obtained. Dowex 50 W-X2 was purchased from Fluka. The resin was converted into the Ca^{2+} form by elution with a 30% $CaCl_2$ solution followed by extensive rinsing with H_2O. NMR spectra were recorded on a Bruker Avance Ultrashield 400 spectrometer (resonance frequencies: 400.13 MHz for ^1H and 100.6 MHz for ^{13}C). Chemical shifts (in ppm) are given relative to either sodium (trimethylsilyl)propionate-d_4 or tetramethylsilane; multiplicities are abbreviated as follows: s = singlet, d = doublet, t = triplet, m = multiplet. C-, H-, and N-analyses were performed by A. Zaschka and H. Feuerhake (Universität des Saarlandes). AAS measurements (determination of *K*) were carried out by T. Allgayer (Prof. H. P. Beck, Universität des Saarlandes).

Potentiometric and Spectrophotometric Titrations. All titrations were carried out at 25 °C at an ionic strength of 0.1 M (KCl) in a batchwise manner.[26] Three independent batches with total vanadium to total ligand (L) molar ratios of 1:3 were performed for each system (L = ino or tmci), and a total of 40 data points was collected for each titration curve ($3.8 < pH < 8.3$ for the vanadium(IV)/ino system and $3.5 < pH < 9.0$ for the vanadium(IV)/tmci system). Each data point corresponded to an individual 10 mL sample that was sealed in a double-jacketed beaker. The samples were allowed to equilibrate for 10−14 days for the vanadium(IV)/ino system and for 8 days for the vanadium(IV)/tmci system. The pH was measured using a Metrohm 780 pH/mV-meter and a Metrohm glass electrode with an internal Ag/AgCl reference. The electrode system was calibrated by acid−base titrations before and after the measurement of each curve. Additionally, UV−vis spectra in the range of 280−1000 nm were recorded for each sample using a diode array spectrophotometer (J&M, Tidas−UV/NIR/100−1) combined with an immersion probe (Hellma). The equilibration time was determined separately by UV−vis spectroscopy for four appropriate sample solutions.

Calculation of Equilibrium Constants. All equilibrium constants were calculated as concentration quotients with $pH = -\log[H^+]$ using the computer program Hyperquad.[27] The pK_w (13.79),[28] and the total concentrations of V, L, and H^+ were treated as fixed values. The hydrolytic species $[VO(OH)]^+$ ($\log \beta_{10-1} = -5.94$),[29] $[(VO)_2(OH)_2]^{2+}$ ($\log \beta_{20-2} = -6.95$),[29] $[VO(OH)_3]^-$ ($\log \beta_{10-3} = -18.0$),[30] and $[(VO)_2(OH)_5]^-$ ($\log \beta_{20-5} = -22.0$)[30] were considered with fixed formation constants. For $[VO(OH)]^+$ and for $[(VO)_2(OH)_2]^{2+}$ the values of the formation constants were adjusted to the appropriate ionic strength by use of the Davies equation.[31] However, all of the simple hydrolytic species do not contribute to any significant extent to the equilibrium composition. In the final evaluation, the three curves of each system were combined to one data set and were evaluated together. The spectroscopic data of the vanadium(IV)/ino system were evaluated using the computer program Specfit.[32] For this purpose, the spectrum of $[VO(H_2O)_5]^{2+}$ was measured separately and imported without refinement. Free ino, $[VO(H_{-3}ino)(OH)_2]^{3-}$, and $[(VO)_2(ino)_2H_{-7}]^{3-}$ were treated as nonabsorbing species. The absorption data considered for evaluation were restricted to the range of $350 < \lambda < 550$ nm.

EPR Measurements. Anisotropic EPR spectra were recorded with an X-band (9.15 GHz) Varian E-9 spectrometer at 120 K. The spectra of the aqueous solutions were measured by dissolving $VOSO_4 \cdot 5H_2O$ and the ligands at the appropriate molar ratio with a concentration of vanadium(IV) of 4 mM. The solutions were stirred and handled under a flow of Ar to avoid the oxidation of vanadium(IV). As usual for low temperature measurements, a few drops of dimethyl sulfoxide (DMSO) were added to the samples to ensure a good glass formation. The spectra of the solid complex $[V(H_{-3}ino)_2][K_2(ino)_2] \cdot 4H_2O$ (**1**) were recorded after dissolution in dimethylformamide (DMF) or $CHCl_3$/toluene 60:40 v/v and without the addition of other solvents. EPR spectra of the non-oxo complexes were simulated with the computer program Bruker WinEPR SimFonia[33] at a microwave frequency of 9.15 GHz. The line widths in the *x*, *y*, and *z* directions were 10, 50, and 10 G, respectively.

Electrochemistry. Cyclic voltammograms (CV) were recorded in 0.5 M KCl, using a BAS C2 cell, a BAS 100B/W potentiostat, a Pt counter electrode, and an Ag/AgCl reference electrode at room temperature (23 ± 3 °C). The pH was adjusted by adding appropriate amounts of a 0.1 M KOH solution. The total vanadium concentration was 4 mM and the total ino concentration was 16 mM. Measurements at positive potentials (V^V/V^{IV} couple) were performed using an Au working electrode. The range with negative potentials (V^{IV}/V^{III} couple) was investigated using a Hg (hanging drop) and a Au working electrode. All potentials were calculated relative to the normal hydrogen electrode (NHE), with a value of +0.46 V for the $[Fe(CN)_6]^{3-/4-}$ couple (0.01 M NaOH).

Preparation of tmci. Both ino (500 mg, 2.78 mmol) and *p*-toluenesulfonic acid monohydrate (150 mg, 0.79 mmol) were suspended in absolute MeOH (30 mL) under N_2, and trimethylorthobenzoate (1.7 eq, 0.8 mL) was added. The mixture was stirred for 16 h and neutralized by the addition of solid K_2CO_3. Volatiles were removed on a rotary evaporator, and the residue was washed with Et_2O. The crude white product, which still contained some *p*-toluenesulfonic acid, was used without further purification (88% yield). Formation of *cis*-inositol-orthobenzoate[34] was established by NMR spectroscopy: ^1H NMR (D_2O): δ 3.93 (m, 3H), 4.32 (m, 3H), 7.50 (m, 3H), and 7.75 (m, 2H). ^{13}C NMR (D_2O): δ 65.9, 79.6, 110.9, 127.9, 131.2, 133.0, and 139.8. For elemental analysis a small sample of the hemihydrate was crystallized from MeOH/

(25) Morgenstern, B.; Sander, J.; Huch, V.; Hegetschweiler, K. *Inorg. Chem.* **2001**, *40*, 5307−5310.
(26) Steinhauser, S.; Heinz, U.; Bartholomä, M.; Weyhermüller, T.; Nick, H.; Hegetschweiler, K. *Eur. J. Inorg. Chem.* **2004**, 4177−4192.
(27) Gans, P.; Sabatini, A.; Vacca, A. *Talanta* **1996**, *43*, 1739−1753.
(28) Smith, R. M.; Martell, A. E.; Motekaitis, R. J. *Critically Selected Stability Constants of Metal Complexes*; NIST Standard Reference Database 46, version 8.0; NIST: Gaithersburg, MD, 2004.
(29) Henry, R. P.; Mitchell, P. C. H.; Prue, J. E. *J. Chem. Soc. Dalton Trans.* **1973**, 1156−1159.
(30) (a) Komura, A.; Hayashi, M.; Imanaga, H. *Bull. Chem. Soc. Jpn.* **1977**, *50*, 2927−2931. (b) Vilas Boas, L. F.; Costa Pessoa J. In *Comprehensive Coordination Chemistry*; Wilkinson, G.; Gillard, R. D.; McCleverty J. A., Eds.; Pergamon Press: Oxford, 1987; Vol. 3, pp 453−583.
(31) Davies, C. W. *J. Chem. Soc.* **1938**, 2093−2098.
(32) (a) Binstead, R. A.; Jung, B.; Zuberbühler, A. D. *SPECFIT/32*, Version 3.0, Spectrum Software Associates: Marlborough, MA 01752, 2000. (b) Gampp, H.; Maeder, M.; Meyer, C. J.; Zuberbühler, A. D. *Talanta* **1985**, *32*, 95−101.
(33) *WINEPR SimFonia*, version 1.25, Bruker Analytische Messtechnik GmbH, Karlsruhe, Germany, 1996.
(34) A corresponding *ortho*-pentanoate has been described. See Biamonte, M. A.; Vasella, A. *Helv. Chim. Acta.* **1998**, *81*, 695−717.

Table 1. Crystallographic Data for **1** and **2**

	1	**2**
chemical formula	$C_{24}H_{50}K_2O_{28}V$	$C_{12}H_{30}Na_6O_{26}S_2V$
fw	915.78	843.36
crystal system	triclinic	trigonal
space group	$P\bar{1}$ (No. 2)	$R\bar{3}$ (No. 148)
a, Å	9.6731(5)	9.5480(10)
b, Å	9.8194(5)	9.5480(10)
c, Å	9.8842(4)	27.314(5)
α, deg	99.394(3)	90.00
β, deg	108.736(2)	90.00
γ, deg	106.614(3)	120.00
V, Å^3	817.63(7)	2156.5(5)
Z	1	3
T, K	100(2)	200(2)
ρ_{calcd}, Mg/m^3	1.860	1.948
μ(Mo−Kα), mm^{-1}	0.675	0.690
reflns (measured, unique, observed)	27708, 8136, 6423	4541, 752, 631
parameters	350	84
R_1, $I > 2\sigma(I)$ [a]	0.0383	0.0557
wR_2 (all data) [b]	0.1024	0.1723

[a] $R_1 = \sum|F_o - F_c|/\sum|F_o|$. [b] $wR_2 = [\sum w(F_o^2 - F_c^2)^2/\sum wF_o^4]^{1/2}$

H_2O. Anal. Calcd for $C_{13}H_{15}O_{6.5}$ (275.26): C, 56.73; H, 5.49. Found: C, 56.84; H, 5.23.

Powdered KOH (3.24 g, 58 mmol) was suspended in 10 mL of DMSO, and the mixture was stirred for 10 min and was cooled with an ice bath. The *cis*-inositol-orthobenzoate (1.28 g, 4.81 mmol) and iodomethane (1.79 mL, 6 eq) were then rapidly added in the order presented. The ice bath was removed and the mixture was stirred for 90 min at room temperature. A concentrated solution of aqueous ammonia (10 mL) was then added and the mixture was stirred for 16 h. The suspension was poured onto 50 mL of water and the mixture was extracted with CH_2Cl_2. After the usual workup, 1,3,5-trideoxy-1,3,5-trimethoxy-*cis*-inositol-orthobenzoate was obtained as a white solid with a yield of 67%. ^{1}H NMR ($CDCl_3$): δ 3.13 (m, 3H), 3.54 (s, 9H), 4.60 (m, 3H), 7.31 (m, 3H), and 7.71 (m, 2H). ^{13}C NMR ($CDCl_3$): δ 56.8, 70.9, 72.7, 107.9, 125.5, 127.7, 129.2, and 137.6.

A portion (900 mg, 2.92 mmol) of 1,3,5-trideoxy-1,3,5-trimethoxy-*cis*-inositol-orthobenzoate was dissolved in a mixture of 5 mL of H_2O and 10 mL of trifluoroacetic acid, and the resulting solution was refluxed for 5 h. After volatiles were removed, the remaining oily residue was ground and washed with Et_2O, which yielded a white solid (87%) that was identified as 2-benzoyl-1,3,5-trideoxy-1,3,5-trimethoxy-*cis*-inositol. ^{1}H NMR (D_2O): δ 3.38 (t, 3H, J = 3 Hz), 3.44 (s, 6H), 3.52 (s, 3H), 3.58 (t, 2H, J = 3 Hz), 4.51 (m, 2H), 6.12 (m, 1H), 7.53 (t, 2H, J = 8 Hz,), 7.67 (t, 1H, J = 8 Hz), and 8.00 (d, 2H, J = 8 Hz). ^{13}C NMR (D_2O): δ 58.8, 59.5, 71.7, 71.8, 79.0, 79.2, 131.7, 131.8, 132.7, 136.9, and 171.1.

The resulting 2-benzoyl-1,3,5-trideoxy-1,3,5-trimethoxy-*cis*-inositol was finally dissolved in aqueous ammonia, and this solution was stirred for 6 days. The reaction mixture was evaporated to dryness, and the resulting residue was dissolved in a small amount of H_2O. This solution was sorbed on a Dowex 50 W (Ca^{2+} form) column. Elution with H_2O yielded a first fraction that consisted of some aromatic side products and unreacted 2-benzoyl-1,3,5-trideoxy-1,3,5-trimethoxy-*cis*-inositol. Pure tmci was obtained as a second fraction, and it was isolated as a white solid after evaporation of the solvent with a yield of 62%. The overall yield as referred to ino was 32% (500 mg). Anal. Calcd for $C_9H_{18}O_6$ (222.24): C, 48.64; H, 8.16. Found: C, 48.52; H, 8.12. ^{1}H NMR (D_2O): δ 3.28 (m, 3H), 3.46 (s, 9H), and 4.46 (m, 3H). ^{13}C NMR (D_2O): δ 58.8, 71.2, and 79.7.

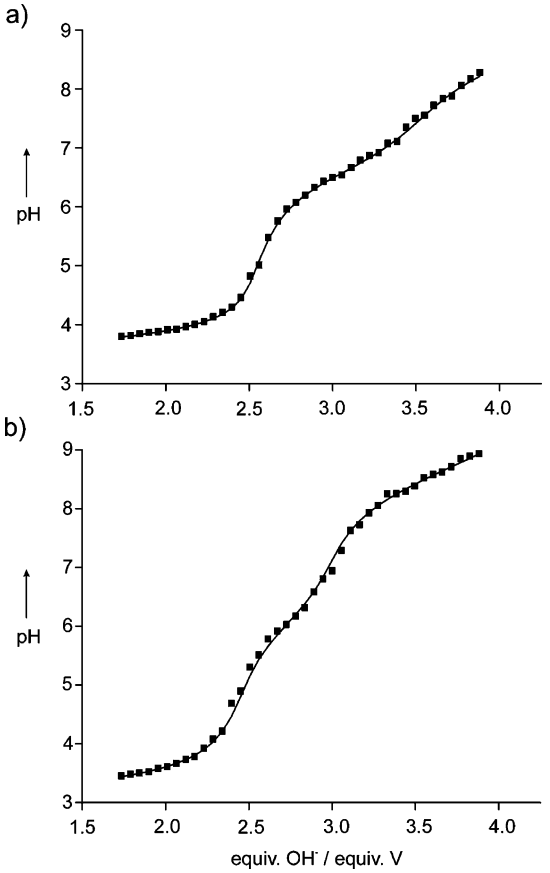

Figure 1. Titration data of a batch experiment a) for the vanadium(IV)/ino system and b) for the vanadium(IV)/tmci system with total vanadium(IV) = 1.5 mM and total L = 4.5 mM (25 °C, 0.1 M KCl). Squares represent experimental values; the fitting curves were calculated using the formation constants evaluated from the potentiometric measurements (Table 2).

Preparation of $[V(H_{-3}ino)_2][K_2(ino)_2]\cdot 4H_2O$ (1). To a solution of ino (200 mg, 1.12 mmol) in H_2O (5 mL), $VOSO_4\cdot 5H_2O$ (142 mg, 0.56 mmol) was added. The resulting blue solution was adjusted to pH ∼ 10 by adding 25 mL of 0.1 M aqueous KOH. A color change to yellow was observed. EtOH (80 mL) was then added to the mixture. A yellow solid (150 mg, 27%) precipitated and was dried on air at room temperature. Anal. Calcd for the octahydrate, $[V(H_{-3}ino)_2]\ [K_2(ino)_2]\cdot 8H_2O$, $C_{24}H_{58}K_2O_{32}V$ (987.84): C, 29.18; H, 5.92. Found: C, 29.20; H, 5.26.

The product was further dried in vacuo, and the resulting yellow powder was suspended in boiling EtOH (50 mL). The mixture was kept under reflux, and small portions of H_2O were added to the mixture until a clear yellow solution was obtained. This solution was allowed to cool at room temperature to yield yellow crystals of **1**, which were dried for a period of 2 days in vacuo. The crystals (45 mg, 49%) were used for the X-ray diffraction study. Anal. Calcd for $C_{24}H_{50}K_2O_{28}V$ (915.78): C, 31.48; H, 5.50; K 8.54. Found: C, 31.70; H, 5.88; K, 8.49.

Preparation of $[Na_6V(H_{-3}ino)_2](SO_4)_2\cdot 6H_2O$ (2). To a solution of ino (100 mg, 0.55 mmol) in H_2O (5 mL), $VOSO_4\cdot 5H_2O$ (71 mg, 0.28 mmol) was added. The resulting blue solution was adjusted to pH ∼ 10 by the addition of 0.5 M aqueous NaOH. A color change to yellow was noted. After the addition of EtOH (5 mL), a yellow solid precipitated, which was isolated by filtration. The solid was exposed to the air at ambient conditions for a few days until a constant weight was reached. Anal. Calcd for the decahydrate, $[Na_6V(H_{-3}ino)_2](SO_4)_2\cdot 10H_2O$, $C_{12}H_{38}Na_6O_{30}S_2V$ (915.43): C, 15.74; H, 4.18. Found: C, 15.79; H, 3.87. The solid was redissolved

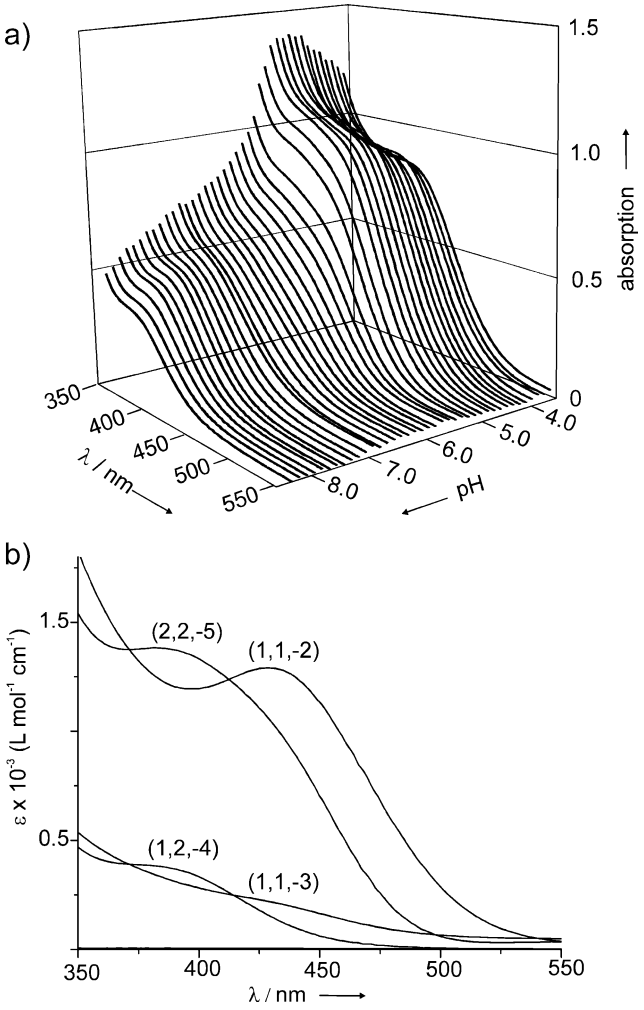

Figure 2. Determination of the formation constants of vanadium(IV)/ino complexes by spectrophotometric batch-titrations. (a) Experimental spectra of the individual sample solutions (corresponding to the points of Figure 1a) with total vanadium(IV) = 1.5 mM and total L = 4.5 mM (25 °C, 0.1 M KCl); (b) calculated spectra of the individual species $[(VO)_xL_yH_z]^{z+2x}$ or $[V_xL_yH_{z-2x}]^{z+2x}$.[36] Absorbance data of VO^{2+} (1,0,0) were measured separately and imported as fixed values; $[VOLH_{-5}]^{3-}$ (1,1,−5), $[(VO)_2(L)_2H_{-7}]^{3-}$ (2,2,−7) and ino (0,1,0) were treated as nonabsorbing species.

in a 1:1 mixture of $EtOH/H_2O$, and the solution was allowed to stand at ambient conditions for a few days. A small amount of yellow crystals of **2** was formed, which was suitable for the X-ray diffraction study.

Crystal Structure Determination. X-ray diffraction data for **1** and **2** were collected at 100(2) and 200(2) K, using a Bruker X8 CCD or a Stoe IPDS diffractometer, respectively. There were 27708 ($2.26 < \Phi < 37.94$) and 4541 ($2.57 < \Phi < 23.89$) reflections collected for the structures **1** and **2**, using graphite-monochromated Mo−Kα radiation ($\lambda = 0.71073$ Å). A compilation of the crystal data is given in Table 1. For both structures, application of an absorption correction proved to not be necessary. The structures were solved using direct methods (SHELXS-97) and refined by full-matrix least-squares calculations on F^2 (SHELXL-97).[35] Anisotropic displacement parameters were used for all non-hydrogen atoms. The hydrogen atoms H1 and H2 of **2** were placed at calculated positions by using a riding model and by isotropic displacement parameters that were fixed at $1.2U_{eq}$ of the corresponding pivot atom. All other hydrogen atoms were located and refined with isotropic displacement parameters. A total of 8136 and 752 unique data were used for the final refinement of 350 and 84 parameters for **1** and **2**, respectively.

(35) (a) Sheldrick, G. M. *SHELXS-97, Program for Crystal Structure Solution*, Göttingen, Germany, 1997. (b) Sheldrick, G. M. *SHELXL-97, Program for Crystal Structure Refinement*, Göttingen, Germany, 1997.

Table 2. Formation Constants log β_{xyz} (25 °C, 0.1 M KCl) of the Vanadium(IV)/ino and the Vanadium(IV)/tmci System as Obtained from Potentiometric and Spectrophotometric Measurements[a,b]

	logβ_{xyz}		
$VO_xL_yH_z/V_xL_yH_{z-2x}$	L = ino		L = tmci
x, *y*, *z*	potent	spectr	potent
1, 1, −2	−5.2(6)	−5.2(3)	−3.6(3)
1, 1, −3	−9.6(2)	−9.9(2)	
2, 2, −5	−10.2(1)	−11.1(2)	−7.9(3)
2, 2, −6			−14.0(3)
1, 2, −4	−14.3(2)	−14.0(2)	−14.3(2)
1, 1, −5	−26.3(2)	−25.3(2)[c]	−26.8(2)
2, 2, −7	−23.8(4)	−25(2)[c]	

[a] Potentiometric = (potent), spectrophotometric = (spectr). [b] $\beta_{xyz} = [(VO)_xL_yH_z] \times [VO]^{-x} \times [L]^{-y} \times [H]^{-z}$ or $[V_xL_yH_{z-2x}] \times [VO]^{-x} \times [L]^{-y} \times [H]^{-z}$. [c] The species was considered as nonabsorbing.

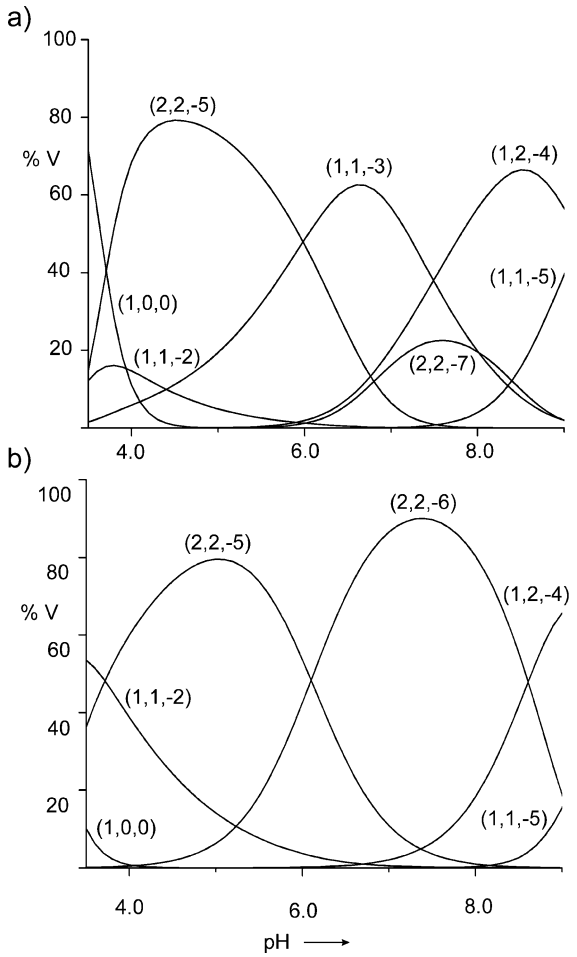

Figure 3. Species distribution in the vanadium(IV)/L system with total vanadium(IV) = 1.5 mM and total L = 4.5 mM (25 °C, 0.1 M KCl); (a) L = ino, (b) L = tmci. The formation constants evaluated from the potentiometric measurements listed in Table 2 were used for the calculations.

(36) Note that only four equivalents of base are required for the deprotonation of the six hydroxy groups according to the reaction $VO^{2+} + 2\ L \rightarrow [V(H_{-3}L)_2]^{2-} + 4\ H^+ + H_2O$ with L = ino, tmci.

Scheme 2. Structure of the Mononuclear Species in the Vanadium(IV)/ino System

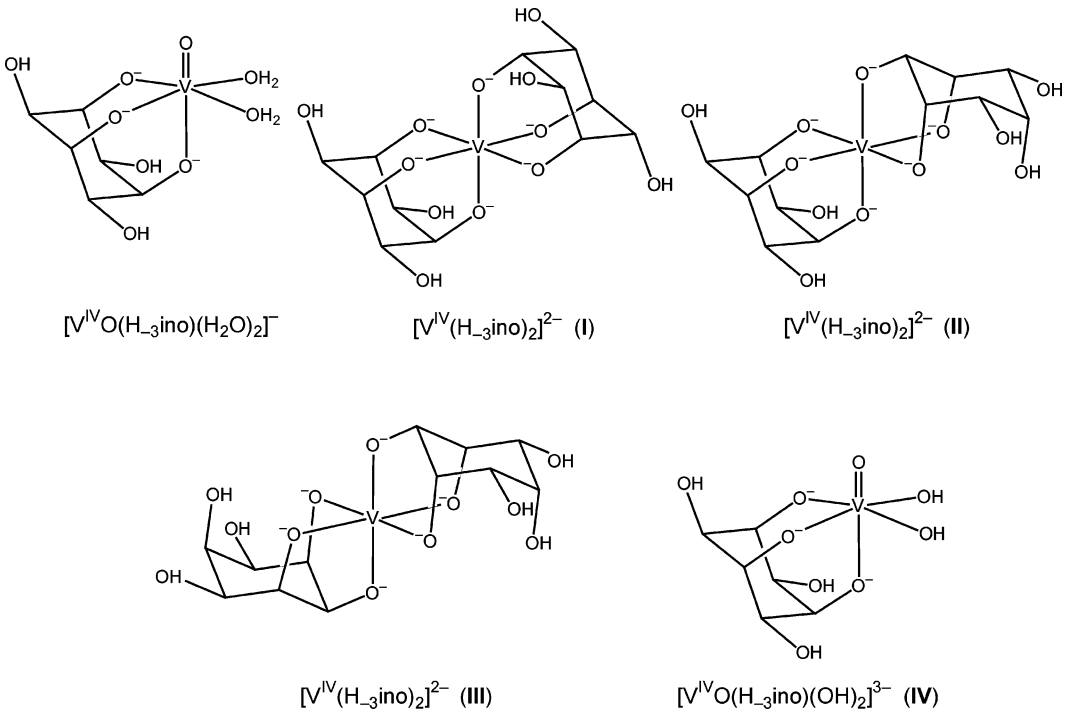

Results and Discussion

Speciation in Aqueous Solution. Complex formation of the vanadium(IV)/ino and vanadium(IV)/tmci systems in aqueous solution was investigated as a function of pH by means of potentiometric titrations. Because of sluggish complex formation and the corresponding long equilibration times, the titration experiments were performed in a batchwise manner. The kinetics of equilibration were followed by UV−vis spectroscopic measurements. However, the reaction proved to be very complex and we are currently far from any conclusive understanding. In the range of 4 < final pH < 6, addition of base to vanadium(IV)/ino samples resulted first in the formation of an almost colorless solution that then turned to a pale yellow within a time span of several days (Figure S1, Supporting Information). The samples with a final pH > 6.5 immediately become a bright yellow after the addition of base. However, this color faded away within 1−2 days. Moreover, UV−vis spectroscopic measurements indicated some additional subsequent changes that could be followed over a time span of several days. The vanadium(IV)/tmci system behaved similarly.

Because the use of glass tubes was problematic at high pH for such a long equilibration time (dissolution of silica) and because the use of plastic ware was also not suitable (slow diffusion of CO_2 through the tube walls) we restricted the pH to a range of about 3.5−9.0 (Figure 1). A total of three independent curves were measured for each system to ensure an unambiguous identification of the various species, and the three curves were combined to form one single data set for evaluation. In addition, the vanadium(IV)/ino system was also investigated by spectrophotometric methods. For each point of the titration curve, an UV−vis spectrum was measured. The spectrophotometric data were evaluated separately (Figure 2) and further corroborated the model established by potentiometric methods. The evaluated formation constants are collected in Table 2, and the species distribution diagrams are shown in Figure 3. The various complexes formed are indicated as (*x*, *y*, *z*), referring to the number of $V^{IV}O$ units (*x*), of ligand entities (ino, tmci) (*y*), and of protons (*z*) that are required for the formation of each species according to the equation

$$x\mathrm{VO}^{2+} + y\mathrm{L} + (-z)\mathrm{OH}^- \rightarrow [(\mathrm{VO})_x\mathrm{L}_y\mathrm{H}_z]^{2x+z} + (-z)\mathrm{H_2O} \quad \text{(i)}$$

and accordingly for the generation of non-oxo species

$$x\mathrm{VO}^{2+} + y\mathrm{L} + (-z)\mathrm{OH}^- \rightarrow [\mathrm{V}_x\mathrm{L}_y\mathrm{H}_{z-2x}]^{2x+z} + (x-z)\mathrm{H_2O} \quad \text{(ii)}$$

Therefore, (1, 0, 0) stands for the aqua cation $[VO(H_2O)_5]^{2+}$, (1, 1, −3) for the complex $[VO(H_{-3}L)]^-$, and (1, 2, −4) for the non-oxo complex $[V(H_{-3}L)_2]^{2-}$.[36]

A tentative structural representation of the mononuclear ino complexes is shown in Scheme 2. The formation of the D_{3d} symmetric (1, 2, −4) species (**I**) has been verified by EPR spectroscopy and by crystal structure analyses of the sodium and potassium salts (vide infra). Compared to the previously described vanadium(IV)/taci system, formation of this particularly interesting non-oxo complex occurred at a higher pH.[15] Because of the 1:1 metal/ligand molar ratio, the dinuclear species (2, 2, −5) and (2, 2, −7) must obviously be interpreted as oxo-complexes. However, bridging via hydroxo and/or by alkoxo groups is possible, and therefore, a structural assignment is thus less conclusive.

According to the spectrophotometric measurements, the non-oxo (1, 2, −4) species (**I**) is primarily formed in freshly prepared solutions and predominates in the pH range 8−13. At high OH^- concentration, however, the potentiometric and spectrophotometric measurements provided ample evidence

Table 3. EPR Parameters of the Vanadium(IV) Complexes of ino, tmci, and Their Derivatives in Aqueous Solution

	g_x	g_y	g_z	A_x [a]	A_y [a]	A_z [a]	$\|A_x - A_y\|$ [a]	ref
$[VO(H_{-3}ino)(H_2O)_2]^-$	1.982	1.982	1.941	61.2	61.2	169.4	0.0	this Work
$[VO(H_{-2}tmci)(H_2O)_2]$	1.981	1.981	1.941	61.8	61.8	169.1	0.0	this Work
$[VO(taci)(H_2O)_2]^{2+}$	1.978	1.978	1.940	61.1	61.1	170.9	0.0	15
$[VO(tdci)(H_2O)_2]^{2+}$	1.981	1.981	1.941	64.2	64.2	171.2	0.0	15
I[b,c]	1.906	1.909	1.986	99.1	96.2	−24.8	2.9	this Work
II[b,d]	1.924	1.920	*g*	98.9	93.3	*g*	5.6	this Work
III[b,e]	1.927	1.922	*g*	∼97	∼90	*g*	∼7	this Work
$[V(H_{-3}tmci)_2]^{2-}$ [c]	1.911	1.916	1.984	100.6	95.8	−23.0	4.8	this Work
$[V(taci)_2]^{4+}$ [c]	1.902	1.907	1.988	99.4	97.2	−16.0	2.2	15
$[V(tdci)_2]^{4+}$ [c]	1.895	1.900	1.988	96.9	94.8	−17.0	2.1	15
IV[f]	*g*	*g*	1.950	*g*	*g*	159.1	*g*	this Work
$[VO(H_{-3}tmci)(OH)_2]^{3-}$	*h*	*h*	1.950	*h*	*h*	159.2	*h*	this Work
$[VO(H_{-3}taci)(OH)_2]^{3-}$	*h*	*h*	1.949	*h*	*h*	160.6	*h*	15
$[VO(H_{-3}tdci)(OH)_2]^{3-}$	*h*	*h*	1.950	*h*	*h*	160.1	*h*	15

[a] Values are measured in units of 10^{-4} cm^{-1}. [b] **I**, **II**, and **III** indicate the three isomers of $[V(H_{-3}ino)_2]^{2-}$ displayed in Scheme 2 (see also Figure 4). [c] bis-(ax−ax−ax) coordination. [d] (ax−ax−ax)−(ax−eq−ax) coordination. [e] bis-(ax−eq−ax) coordination. [f] **IV** in Scheme 2 (see also Figure 5). [g] Parameters not measurable due to the presence of the non-oxo complex **I**. [h] Parameters not measurable due to the presence of the non-oxo complex.

that, at room temperature, this non-oxo complex slowly transforms into a colorless species of composition (1, 1, −5) within a time period of several days. We tentatively assign the oxo-dihydroxo structure $[VO(H_{-3}ino)(OH)_2]^{3-}$ to this species (**IV** in Scheme 2).

The species distribution of the vanadium(IV)/tmci system is generally similar to the vanadium(IV)/ino system (Table 2 and Figure 3b). Remarkable differences are (i) the dinuclear nature of the complex (1, 1, −3) which was observed as (2, 2, −6) for tmci (Table 2 and Figure 3), and (ii) the non-observance of a (2, 2, −7) species.

EPR Spectroscopy in Aqueous Solution. The complexation scheme elucidated by potentiometry and spectrophotometry was substantiated by EPR measurements. The spectra of the vanadium(IV)/ino system recorded in aqueous solution with a total vanadium:total ino ratio of 1:2 and a vanadium(IV) concentration of 4 mM indicated formation of the $[(VO)_2(ino)_2H_{-5}]^-$, $[VO(H_{-3}ino)]^-$, $[(VO)_2(ino)_2H_{-7}]^{3-}$, $[V(H_{-3}ino)_2]^{2-}$, and $[VO(H_{-3}ino)(OH)_2]^{3-}$ species. In aqueous solution below pH 4, vanadium(IV) exists as the pale blue aqua ion $[VO(H_2O)_5]^{2+}$. In the pH range 4−5 a significant weakening of the EPR signal was observed, which suggests the presence of a di- or a polynuclear species. These findings were confirmed by the measurements at pH ∼ 5 of an equimolar solution with vanadium(IV) and ino concentrations of 10 or 50 mM, which favored the formation of the dinuclear complex (Figure S2, Supporting Information). Anisotropic EPR spectra showed a broad unresolved absorption centered at $g = 2.098$ in the $\Delta M = \pm 1$ region and a forbidden signal at 1550 G in the $\Delta M = \pm 2$ region. No indications for monomeric species were verified in the concentrated solutions. All of these features support a dinuclear arrangement and a ferromagnetic interaction between the two $V^{IV}O$ ions,[37] with an alkoxo or hydroxo bridged structure such as those formed, for example, by ino with Fe^{III} [24] and by taci with Pb^{II},[38] Bi^{III},[38] La^{III},[39] and Gd^{III}.[39]

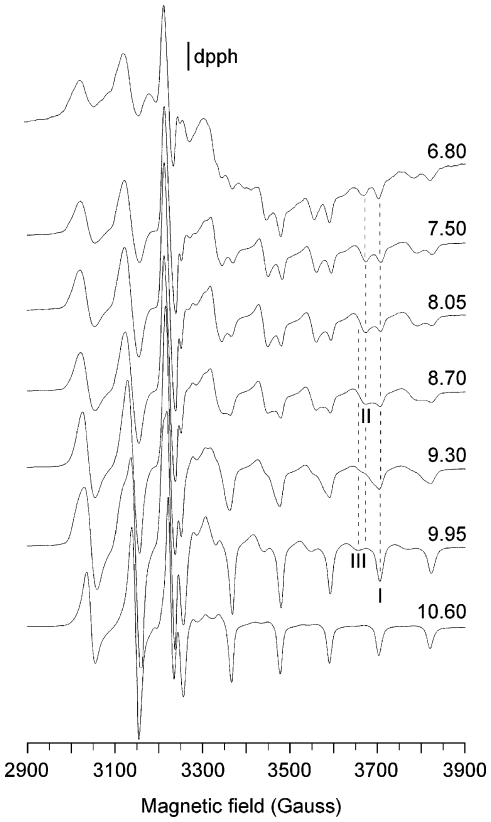

Figure 4. X-band anisotropic EPR spectra as a function of the pH at 140 K in the vanadium(IV)/ino system with total vanadium(IV) = 4 mM and total ino = 40 mM. **I**, **II**, and **III** indicate the resonances of the three isomers of $[V(H_{-3}ino)_2]^{2-}$ with bis-(ax−ax−ax), (ax−ax−ax)−(ax−eq−ax), and bis-(ax−eq−ax) coordination mode, respectively (see Scheme 2). Diphenylpicrylhydrazyl (dpph) was used as standard field marker ($g_{dpph} = 2.0036$).

In the pH range 5.5−7 formation of $[VO(H_{-3}ino)(H_2O)_2]^-$, which has two water molecules in the cis position to the V=O bond, occurred (Scheme 2). The experimental EPR parameters (Table 3) are comparable to those of the corresponding taci and tdci complexes,[15] and they are consistent with the additivity rule used for calculating the parallel hyperfine coupling constant with the ^{51}V nucleus.[40] The ground state is d_{xy}, as is expected for a $V^{IV}O$ complex.

Anisotropic EPR spectra of the non-oxo complex $[V(H_{-3}ino)_2]^{2-}$ are shown in Figure 4 as a function of pH.

(37) Smith, T. D.; Pilbrow, J. R. *Coord. Chem. Rev.* **1974**, *13*, 173−278.
(38) Hegetschweiler, K.; Ghisletta, M.; Gramlich, V. *Inorg. Chem.* **1993**, *32*, 2699−2704.
(39) Hedinger, R.; Ghisletta, M.; Hegetschweiler, K.; Tóth, E.; Merbach, A. E.; Sessoli, R.; Gatteschi, D.; Gramlich, V. *Inorg. Chem.* **1998**, *37*, 6698−6705.

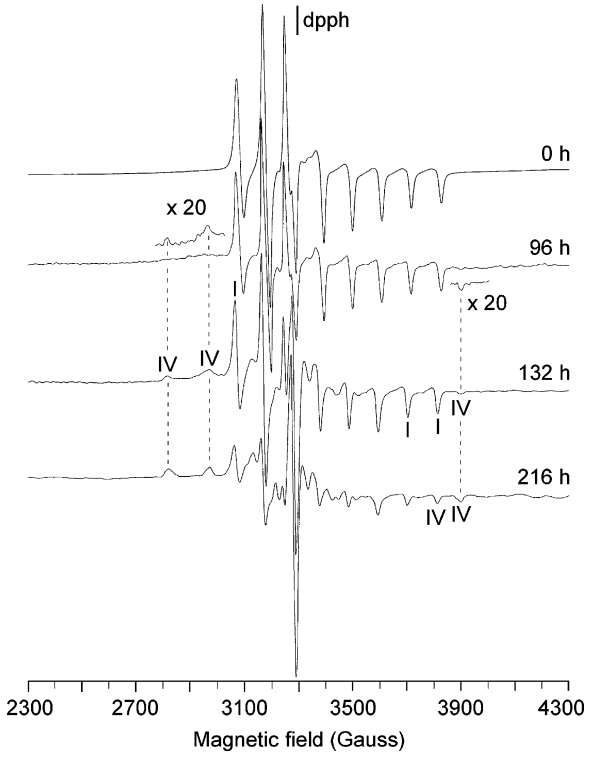

Figure 5. X-band anisotropic EPR spectra as a function of the time at pH 10.5 and at 140 K in the vanadium(IV)/ino system with total vanadium(IV) = 4 mM and total ino = 8 mM. **I** and **IV** indicate the resonances of $[V(H_{-3}ino)_2]^{2-}$ (1,2,−4) and $[VO(H_{-3}ino)(OH)_2]^{3-}$ (1,1,−5), respectively (see Scheme 2). Diphenylpicrylhydrazyl (dpph) was used as standard field marker (g_{dpph} = 2.0036).

At a total ino:total vanadium ratio of 2:1 or higher, three sets of resonances (**I**, **II**, and **III** in Figure 4), belonging to three distinct non-oxo species (**I**, **II**, and **III** in Scheme 2), are observed simultaneously between pH 7 and 11. However, due to the weak intensity of the signals attributable to the species **III**, only approximate parameters can be extracted, and the g_z and A_z values cannot be measured (Table 3). On the basis of the EPR properties displayed by the solid samples (vide infra) and in agreement with the corresponding parameters of the analogous taci and tdci complexes,[15] species **I** was identified as a double-adamantane type complex with a D_{3d} symmetry and a bis-(ax−ax−ax) structure (Scheme 2). Because the resonances of **II** and **III** are clearly characteristic of non-oxo species as well, an isomerism between the complexes with (ax−ax−ax)−(ax−eq−ax) and bis-(ax−eq−ax) coordination mode was postulated for these species. In agreement with the above-mentioned steric requirements,[22] the stability of the isomers **II** and **III**, which have either one or two (ax−eq−ax) arrangements of the ligand molecules, is decreasing. The increase of the $|A_x - A_y|$ value from the isomer **I** to **III** is also in agreement with a progressive distortion of the pseudo-octahedral geometry. The equilibrium between the three species was found to be dependent on pH: with increasing pH, the minor components **II** and **III** disappeared, and only the isomer **I** with the bis-(ax−ax−ax) structure was detected above pH 11 (Figure S3, Supporting Information). As expected for a rapid equilibrium, the ratio of the three components did not depend on the age of the samples and remained constant over a period of several days (Figure S4, Supporting Information).

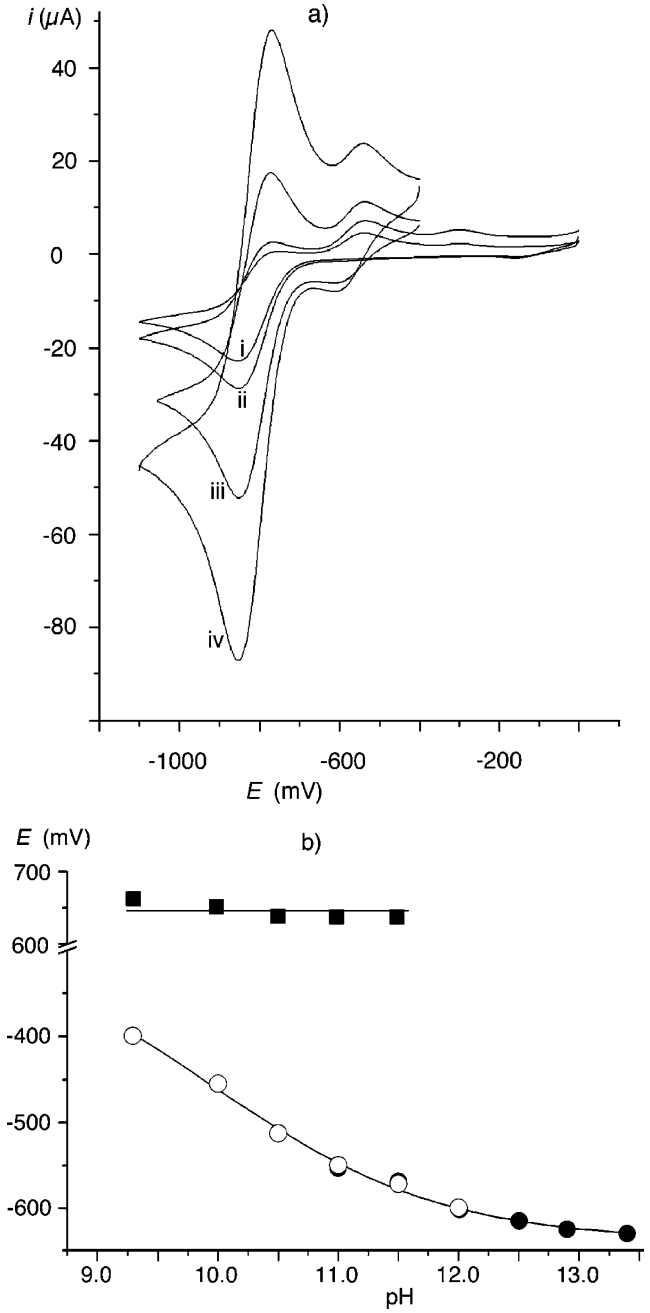

Figure 6. Cyclic voltammetric measurements of $[V(H_{-3}ino)_2]^{2-}$. (a) Cyclic voltammograms of the $[V^{IV/III}(H_{-3}ino)_2]^{2-/3-}$ couple at pH 11.0 as a function of the scan rate: (i) 50 mV/s; (ii) 100 mV/s; (iii) 600 mV/s and (iv) 2000 mV/s (*E* vs Ag/AgCl-reference). (b) pH dependence of the midpoint potentials of $[V^{V/IV}(H_{-3}ino)_2]^{-/2-}$ (squares) and $[V^{IV/III}(H_{-3}ino)_2]^{2-/3-}$ (circles). Closed circles show the potentials (vs NHE) measured with an Au-working electrode and open circles are those measured with a Hg (hanging drop) electrode.

As mentioned in the introduction, an (ax−eq−ax) coordination of ino has previously been observed in the solid-state structure of $K_5[OFe_6(ino)_6H_{-21}]$.[24] Furthermore, a corresponding isomerization reaction between the two modes (ax−ax−ax) and (ax−eq−ax) has been elucidated for

(40) Chasteen, N. D. In *Biological Magnetic Resonance*; Berliner, L. J.; Reuben, J., Eds.; Plenum Press: New York, 1981; Vol. 3, pp 53−119.

Table 4. Summary of Selected Bond Distances (Å) for the Complexes **1** and **2**

	1			**2**		
	min	max	average	min	max	average
$V-O_{alkoxo}$	1.9023(8)	1.9260(7)	1.9159			1.861(3)
$Na-O_{sulfato}$				2.319(4)	2.606(4)	2.431
$Na-O_{alkoxo}$				2.350(4)	2.397(4)	2.378
$K-O_{alkoxo}$	2.7118(9)	3.0050(9)	2.7938			
$K-OH_2$(term)			2.8482(9)			
C−O	1.4172(13)	1.4317(13)	1.4241	1.421(5)	1.439(6)	1.430
C−C	1.5262(17)	1.5348(15)	1.5300	1.537(7)	1.538(7)	1.538

$[Co^{III}(tach)(H_{-x}ino)]^{(3-x)}$ by means of ^1H NMR spectroscopy (tach = cyclohexane-1,3,5-triamine).[41] It is thus not too surprising that vanadium(IV), having an ionic radius (0.58 Å) between high-spin Fe^{III} (0.65 Å) and low-spin Co^{III} (0.55 Å),[23] exhibits an analogous behavior.

To confirm this hypothesis, the vanadium(IV)/tmci system has been included in our study. As noted above in Scheme 1, the coordination mode of this ligand is restricted to (ax−ax−ax). The complexation process displayed by tmci is substantially comparable with that of ino. EPR spectra recorded as a function of pH with total tmci:total vanadium ratios of 2:1 or 10:1 showed the formation of $[VO(H_{-2}tmci)]$ in weakly acidic solution, of di- or polynuclear species around neutrality, of a non-oxo $[V(H_{-3}tmci)_2]^{2-}$ complex in the pH range 9−10, and of $[VO(H_{-3}tmci)(OH)_2]^{3-}$ in very basic solution. It is noteworthy that with tmci only one non-oxo vanadium(IV) species was observed between pH 7 and 11 (Figure S5, Supporting Information). The spectrum of the D_{3d} symmetric $[V(H_{-3}tmci)_2]^{2-}$ (Figure S6, Supporting Information) has been simulated and the parameters, which are comparable to those displayed by non-oxo complexes of taci, tdci, and ino, are reported in Table 3.

As mentioned above, the potentiometric and spectrophotometric measurements provided evidence that above pH 10 $[V(H_{-3}ino)_2]^{2-}$ is slowly converted into a colorless $V^{IV}O$ species within a period of several days. This transformation can also be followed by EPR spectroscopy. In Figure 5, the resonances of **IV**, which are superimposed to those of the non-oxo complex **I** (see Scheme 2 and Figure 4), are indicated by dotted lines. EPR parameters ($g_z < g_x \sim g_y$ and $A_z > A_x \sim A_y$) are characteristic of a "normal" $V^{IV}O$ species with tetragonal symmetry (Table 3).[40] In analogy to $[VO(H_{-3}taci)(OH)_2]^{3-}$ and $[VO(H_{-3}tdci)(OH)_2]^{3-}$, two of the alkoxo groups of ino occupy cis positions and one of them the trans position with respect to the V=O bond. The two additional OH^- ligands are in the remaining cis positions (Scheme 2).[15] Analogous behavior is observed in the vanadium(IV)/tmci system, where the corresponding $[VO(H_{-3}tmci)(OH)_2]^{3-}$ complex is formed (Table 3).

Electrochemistry. In freshly prepared, strongly alkaline solutions, cyclic voltammetric measurements established two major one-electron transitions, which correspond to a reduction and an oxidation of the $[V^{IV}(H_{-3}ino)_2]^{2-}$ complex. For both processes, the anodic peak current depended in a strictly linear fashion on the square root of the scan rate, indicating thus a diffusion controlled electron-transfer reaction. However, in agreement with the above-mentioned slow formation of oxo species such as (2, 2, −7) and (1, 1, −5), an aging process was observed for these samples, and after a waiting time of a few days the cyclic voltammograms did not reveal any interpretable signals.

The reduction of $[V^{IV}(H_{-3}ino)_2]^{2-}$ was observed at strongly negative potentials. At low scan rates (<100 mV/s), the measurements indicated a partially irreversible process with one single reduction wave and a series of several oxidation waves (Figure 6a). This observation is indicative of a slow decomposition/rearrangement of the complex at the vanadium(III) stage. At higher scan rates (>600 mV/s), the observed pattern can be assigned to the quasi reversible redox reactions of a major and a minor component, with the midpoint potential $E_{1/2}$ of the minor component appearing as a slightly less negative potential. A possible explanation for this observation would be the binding of the vanadium(III) and vanadium(IV) center to different alkoxo groups ((ax−eq−ax) vs (ax−ax−ax) coordination) of an ino molecule (Schemes 1 and 2). This observation is in agreement with the EPR measurements, where also more than two non-oxo vanadium(IV) complexes were detected for $[V^{IV}(H_{-3}ino)_2]^{2-}$ in basic solutions. Below pH 9, the EPR data indicate formation of three different isomers of the $[V^{IV}(H_{-3}ino)_2]^{2-}$ species at comparable portions. In agreement with these findings, these CVs were exceedingly complex, and a straightforward interpretation proved to be not possible. Interestingly, a corresponding minor transition was not observed for the $[V^{IV/III}(H_{-3}tmci)_2]^{2-/3-}$ complexes where the three equatorial methylated oxygen donors cannot be coordinated to the metal center.

The peak separation for the V^{IV}/V^{III} couple remains approximately constant at 80−90 mV up to a scan rate of 2000 mV/s. The midpoint potential, $E_{1/2}$, of this couple is, however, pH-dependent, and it increases with decreasing pH (Figure 6b). Such a behavior can be explained by the possible protonation of a coordinated alkoxo group at the vanadium(III) stage, favored by the lower charge on the metal center.

$$[V^{IV}(H_{-3}ino)_2]^{2-} + e^- + H^+ \rightarrow [V^{III}(H_{-3}ino)(H_{-2}ino)]^{2-} \quad \text{(iii)}$$

Above pH ∼ 13, $E_{1/2}$ remains constant and the reaction occurs according to the following equation:

$$[V^{IV}(H_{-3}ino)_2]^{2-} + e^- \rightarrow [V^{III}(H_{-3}ino)_2]^{3-} \quad \text{(iv)}$$

(41) Hausherr-Primo, L.; Hegetschweiler, K.; Rüegger, H.; Odier, L.; Hancock, R. D.; Schmalle, H. W.; Gramlich, V. *J. Chem. Soc. Dalton Trans*. **1994**, 1689−1701.

A value of −0.64 V (vs NHE) was assigned to the reduction potential ($E_{1/2}$) of the major component (D_{3d} isomer, **I** in Scheme 2 and Figure 4) in the latter process.

The oxidation of $[V^{IV}(H_{-3}ino)_2]^{2-}$ occurred at a potential of +0.64 V (vs NHE), and it did not show any significant pH dependence between pH 10 and 13.5 (Figure 6b). Obviously, the V^{IV} and V^{V} *cis*-inositolato complexes cannot be protonated under these conditions:

$$[V^{IV}(H_{-3}ino)_2]^{2-} \rightarrow [V^{V}(H_{-3}ino)_2]^{-} + e^{-} \qquad (v)$$

The quasi reversible electron transfer of this process showed a constant peak separation of 70−80 mV for scan rates in the range 20−2000 mV/s, which increased to a value of 120 mV for a scan rate of 5000 mV/s.

Crystal Structures. As seen in the previous sections, the clear yellow aqueous solutions, which are obtained by the combination of $VOSO_4 \cdot 5H_2O$ and ino in a 1:2 molar ratio at a high pH, contain the mononuclear non-oxo species $[V(H_{-3}ino)_2]^{2-}$. Corresponding single crystals of composition $[V(H_{-3}ino)_2][K_2(ino)_2] \cdot 4H_2O$ (**1**) and $[Na_6V(H_{-3}ino)_2](SO_4)_2 \cdot 6H_2O$ (**2**) could be grown readily from these solutions, using either KOH or NaOH as base, respectively. In both compounds **1** and **2**, an almost exactly octahedral coordination sphere is observed for the vanadium(IV) centers. Because of the crystallographically imposed site symmetry ($\bar{1}$ for **1** and $\bar{3}$ for **2**), the coordination geometry is centrosymmetric and corresponds to a trigonal antiprism with a twist angle (Φ) of 60°. These values correspond to the ideal angle that is expected for a regular octahedron. Similar twist angles were also observed for the analogous complexes formed by taci and tdci.[15,42] Furthermore, the difference for interligand and intraligand O···O distances is negligible (2.71/2.70 Å for **1** and 2.66/2.60 Å for **2**). The $V-O_{alkoxo}$ bond distances of the potassium derivative **1** fall in the range of 1.90−1.93 Å (Table 4). These values are in good agreement with the previously described structures and clearly indicate a +IV valence state for the vanadium center. The corresponding $V-O_{alkoxo}$ distance in the trigonal sodium derivative **2** (1.86 Å) is remarkably short, but the EPR study clearly established that vanadium is present in the vanadium(IV) state. Moreover, the redox potential that has been determined for the corresponding V^{IV}/V^{V} couple (Figure 6) is rather high, and a spontaneous oxidation is therefore unlikely. The vanadium(IV) state is also in agreement with charge-balance considerations (the six coordinated alcoholic oxygen donors are all deprotonated).

The $[V(H_{-3}ino)_2]^{2-}$ anion can be regarded as a D_{3d} symmetric rod having a bipolar shape; the six coordinated and deprotonated alkoxo groups together with the six non-coordinating hydroxy groups form a hydrophilic equator, whereas the outside of the two cyclohexane residues represent two hydrophilic poles. As such rods, these units can serve as interesting building blocks for a supramolecular solid-state architecture. The alkoxo and hydroxo groups of a *cis*-inositolato complex can either undergo multiple hydrogen bonding interactions or bind additional cations.[24,25] Interestingly, both concepts are realized in the structures of **1** and **2**: in the potassium derivative **1**, a complex network of hydrogen bonds is formed, and as a consequence, the rotational symmetry observed for isolated $[V(H_{-3}ino)_2]^{2-}$ units is not preserved within the crystal structure; in the sodium complex **2**, a total of six Na^+ cations are coordinated to the alkoxo groups, leading to a $[Na_6V(H_{-3}ino)_2]^{4+}$ cation that retains its threefold rotational symmetry.

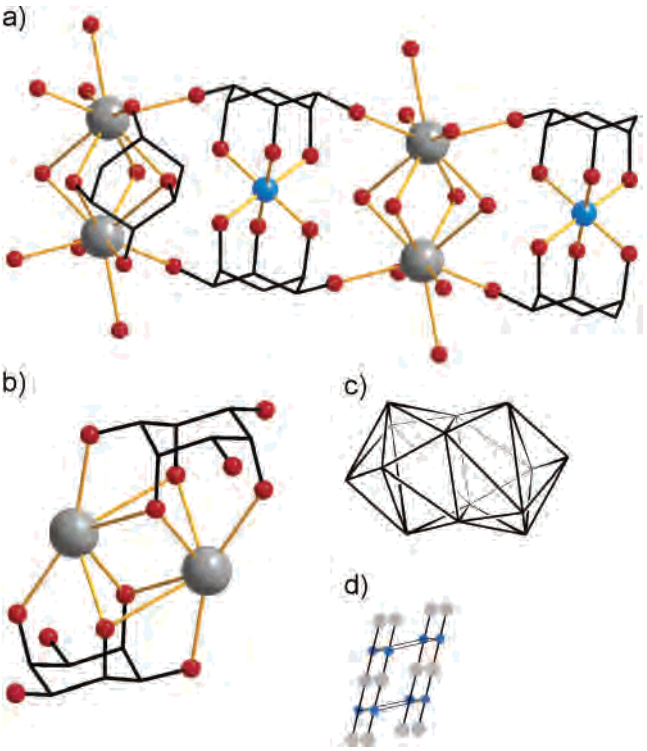

Figure 7. Crystal structure of **1**. (a) Section of one of the chains aligned along the *c*-axis, consisting of an alternating arrangement of $[V(H_{-3}ino)_2]^{2-}$ anions and $[K_2(ino)_2]^{2+}$ cations. Only the K_2O_{14} part of the cations is shown, and non-coordinating hydroxy groups of the anions are omitted for clarity. In the cation on the left side one cyclohexane backbone of an ino ligand is shown. Hydrogen atoms are omitted for clarity. Color code: V, blue; O, red; K, gray; the carbon skeleton is shown as a stick model in black. (b) Structure of the centrosymmetric $[K_2(ino)_2]^{2+}$ cation. (c) Coordination spheres of the K^+ centers. (d) Representation of the packing ($[V(H_{-3}ino)_2]^{2-}$ anions in blue and $[K_2(ino)_2]^{2+}$ cations in gray).

The crystal structure of the potassium complex **1** corresponds to an unusual 1:1 packing of $[V(H_{-3}ino)_2]^{2-}$ dianions and $[K_2(ino)_2]^{2+}$ dications (Figure 7). The anions and cations form linear chains along the crystallographic *c*-axis. Each anion−cation interaction comprises two equatorial hydroxy groups of a $[V(H_{-3}ino)_2]^{2-}$ anion which coordinate a K^+ center of the neighboring cation. Notably, these chains are stacked in an eclipsed rather than a staggered arrangement with short anion−anion and cation−cation separations on the one hand and long cation−anion separations on the other. This type of packing, not known for simple ionic solids, clearly shows that the structure is mainly held together by hydrogen bonding interactions and not by the electrostatic

(42) A re-examination of the twist angles of $[V^{IV}(taci)_2]^{4+}$ and $[V^{IV}(tdci)_2]^{4+}$ reported in ref 15 for the crystal structures of $[V^{IV}(taci)_2](SO_4)_2 \cdot 12H_2O$, $[V^{IV}(tdci)_2][V_4{}^{V}O_{12}] \cdot 14.5H_2O$, and $[V^{IV}(tdci)_2H_{-1}]Cl_3 \cdot 15H_2O$ revealed a value of 59.5° for the taci complex and a value of exactly 60.0° for the two centrosymmetric tdci complexes, provided that the two triangles oriented perpendicular to the (pseudo) threefold rotational axis are considered.

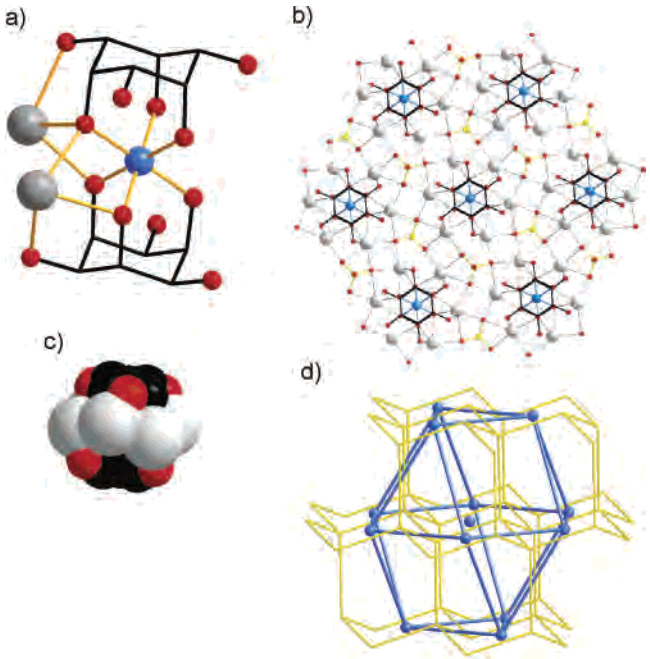

Figure 8. Crystal structure of **2**. (a) The $[V(H_{-3}ino)_2]^{2-}$ anion together with two of the six Na^+ ions which surround the equator of the anion. Hydrogen atoms are omitted for clarity. Color code: V, blue; O, red; Na, gray; the carbon skeleton is shown as a stick model in black. (b) View on a layer, oriented parallel to the *ab*-plane (sulfur atoms of the SO_4^{2-} anions in yellow). (c) space filling model of the entire, S_6 symmetric $[Na_6V(H_{-3}ino)_2]^{4+}$ cation. (d) Section of the three-dimensional network that can be derived from a face centered cubic packing of the $[Na_6V(H_{-3}ino)_2]^{4+}$ cations (shown as blue spheres) with the sulfate counterions (yellow) in the tetrahedral holes of this packing.

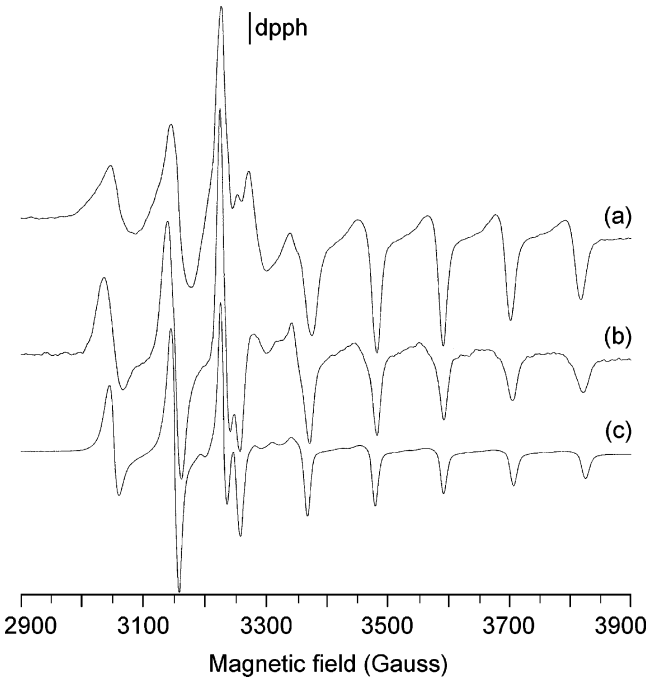

Figure 9. X-band anisotropic EPR spectra at 140 K of the $[V(H_{-3}ino)_2]^{2-}$ anion in several solvents. (a) DMF; (b) $CHCl_3$/toluene 60:40 v/v; (c) aqueous solution at pH 10.85 with total vanadium(IV) = 4 mM and total ino = 8 mM. (a) and (b) were recorded after dissolution of **1** in DMF or in $CHCl_3$/toluene 60:40 v/v. Diphenylpicrylhydrazyl (dpph) was used as standard field marker ($g_{dpph} = 2.0036$).

forces between the differently charged ions. The molecular structure of the $[K_2(ino)_2]^{2+}$ dication with both K^+ ions bonded simultaneously to an (ax−eq−ax) and an (ax−ax−ax) site of the ino ligands is unprecedented.[16] The cations lie on centers of inversion; they approach, however, C_{2h} molecular symmetry quite closely. In addition to the six alcoholic donor groups of the two ino ligands and the two above-mentioned hydroxy groups of the neighboring anion, each K^+ center is coordinated to a H_2O molecule, arriving thus to a coordination number of nine. Four of the eight coordinated alcoholic OH donors of $[K_2(ino)_2]^{2+}$ serve as μ-ROH bridges, and they form a slightly elongated square. The coordination spheres of the two K^+ centers can thus be described as two slightly distorted, mono capped square antiprisms which share the $(\mu$-ROH$)_4$-square. Such a dimeric structure is rather unusual for K^+. We are only aware of one additional example (a K−Ti calix[4]arene dimer) where two fused, mono-capped antiprisms have a square face in common.[43] In this K−Ti calix[4]arene dimer, the K···K separation is 4.78 Å, whereas in $[K_2(ino)_2]^{2+}$ it is 3.64 Å. This relatively short K···K distance is clearly a consequence of the high rigidity of the ino ligand. A related short K···K distance (3.51 Å) is observed for K_2ZrF_6, where two nine-coordinate K^+ centers also share their coordination polyhedra (strongly distorted monocapped cubes) by a common square face.[44]

Compound **2** crystallizes in the rhombohedral space group $R\bar{3}$ with the $[V(H_{-3}ino)_2]^{2-}$ anion lying on threefold rotational inversion (S_6) axes (Figure 8). The $[V(H_{-3}ino)_2]^{2-}$ complex is surrounded by six Na^+ counterions that are bonded to the axial alkoxo oxygens and to the equatorial hydroxy oxygens of the *cis*-inositolato moieties. The alkoxo oxygens undergo Na−O−Na bridging, whereas the hydroxy groups coordinate in a terminal fashion. As a result of the interaction with the equatorial hydroxy groups, the six sodium ions adopt a puckered ring structure with a chair conformation and a Na···Na distance of 3.33 Å. The Na−O distances are in good agreement with the literature values (Table 4).[45] This puckering destroys the pseudo-mirror plains of the D_{3d} symmetric $[V(H_{-3}ino)_2]^{2-}$ core, and as a consequence, the symmetry of the entire $[Na_6V(H_{-3}ino)_2]^{4+}$ entity is S_6. The six Na^+ centers are further interlinked by six sulfate moieties forming in turn either OS-$(\mu_3$-O$)_3$ bridges or undergo bidentate chelation. The SO_4^{2-} units are again placed on threefold rotational axes, and as a consequence, each of them coordinates a total of three $[Na_6V(H_{-3}ino)_2]^{4+}$ entities (Figure 8b). The interlinking of $[V(H_{-3}ino)_2]^{2-}$ anions, Na^+ cations, and SO_4^{2-} counterions results in the formation of a two-dimensional network that is oriented parallel to the crystallographic *ab*-plane. It is noteworthy that only three oxygen atoms of the sulfate unit are incorporated in this network;

(43) Petrella, A. J.; Craig, D. C.; Lamb, R. N.; Raston, C. L.; Roberts, N. K. *Dalton Trans.* **2003**, 4590−4597.
(44) Bode, H.; Teufer, G. *Acta. Crystallogr.* **1956**, *9*, 929−933.
(45) (a) Armstrong, D. R.; Clegg, W.; Drummond, A. M.; Liddle, S. T.; Mulvey, R. E. *J. Am. Chem. Soc.* **2000**, *122*, 11117−11124. (b) Geier, J.; Grützmacher, H. *Chem. Commun.* **2003**, 2942−2943. (c) Geier, J.; Rüegger, H.; Grützmacher, H. *Dalton Trans.* **2006**, 129−136. (d) Fischer, R.; Görls, H.; Walther, D. *Eur. J. Inorg. Chem.* **2004**, 1243−1252. (e) MacDougall, D. J.; Noll, B. C.; Henderson, K. W. *Inorg. Chem.* **2005**, *44*, 1181−1183.

Table 5. EPR Parameters of Non-Oxo Vanadium(IV) Complexes of ino and Its Derivatives in Several Solvents

	solvent	g_x	g_y	g_z	A_x [a]	A_y [a]	A_z [a]	$\lvert A_x - A_y \rvert$ [a]
$[V(H_{-3}ino)_2]^{2-}$	H_2O	1.906	1.909	1.986	99.1	96.2	−24.8	2.9
$[V(H_{-3}ino)_2]^{2-}$ [b]	DMF	1.911	1.915	*e*	100.7	94.2	*e*	6.5
$[V(H_{-3}ino)_2]^{2-}$ [b]	$CHCl_3$/toluene 60:40 v/v	1.910	1.913	1.988	99.2	94.2	−26.8	5.0
$[V(taci)_2]^{4+}$	H_2O	1.902	1.907	1.988	99.4	97.2	−16.0	2.2
$[V(taci)_2]^{4+}$ [c]	DMF	1.904	1.907	*e*	98.5	96.0	*e*	2.5
$[V(taci)_2]^{4+}$ [c]	$CHCl_3$/toluene 60:40 v/v	1.903	1.906	1.987	99.8	96.7	−18.6	3.1
$[V(tdci)_2]^{4+}$	H_2O	1.895	1.900	1.988	96.9	94.8	−17.0	2.1
$[V(tdci)_2]^{4+}$ [d]	DMF	1.894	1.892	*e*	101.0	91.8	*e*	9.2
$[V(tdci)_2]^{4+}$ [d]	$CHCl_3$/toluene 60:40 v/v	1.892	1.893	1.988	101.1	92.2	−19.8	8.9

[a] Values are measured in units of 10^{-4} cm^{-1}. [b] Spectrum obtained after dissolution of **1** in the solvent or in the mixture of solvents. [c] Spectrum obtained after dissolution of $[V^{IV}(taci)_2](SO_4)_2 \cdot 12H_2O$ in the solvent or in the mixture of solvents. [d] Spectrum obtained after dissolution of $[V^{IV}(tdci)_2][V^{V}_4O_{12}] \cdot 14.5H_2O$ in the solvent or in the mixture of solvents. [e] Parameters not measurable for the poor resolution of the spectrum.

the fourth oxygen atom is placed either directly above or directly beneath its parent sulfur atom and is not involved in any binding interaction at all.

The $[Na_6V(H_{-3}ino)_2]^{4+}$ cations, which have an almost spherical shape (Figure 8c), approximately adopt a closed sphere packing with the sulfate counterions located in the tetrahedral holes of this packing. The crystal structure of **2** can thus be derived from the anti-CaF_2 structure type (space group $Fm\bar{3}m$) by a series of group−subgroup relations, namely, (a) a stretching of the structure along the trigonal axis ($Fm\bar{3}m \rightarrow R\bar{3}m$) and (b) the above-mentioned loss of mirror planes ($R\bar{3}m \rightarrow R\bar{3}$) due to the nonplanar arrangement of the Na^+ ions. As a consequence, each $[Na_6V(H_{-3}ino)_2]^{4+}$ cation is surrounded by 12 additional cations, and the stretching along the trigonal axis is indicated by two slightly different edge lengths (10.64 and 9.55 Å) of the corresponding cube octahedron (Figure 8d).

EPR Characterization of Non-oxo Complexes in Weakly Coordinating Solvents. Six-coordinate vanadium(IV) complexes can be divided into two groups: (i) those with a d_{xy} ground state, and $g_z \ll g_x \sim g_y < 2.0023$ and $A_z \gg A_x \sim A_y$; and (ii) those with a d_{z^2} ground state, and $g_x \sim g_y \ll g_z \sim 2.0023$ and $A_z \ll A_x \sim A_y$.[46] On the basis of the experimental parameters (Table 3), the non-oxo complexes of ino and tmci belong to the second group and have a d_{z^2} ground state. In the literature, it is proposed that this electronic configuration characterizes hexa-coordinated vanadium(IV) species with a geometry distorted toward a trigonal prism.[46−48]

In accordance with similar observations, reported recently for $[V(taci)_2]^{4+}$ and $[V(tdci)_2]^{4+}$ cations,[15] the anomaly of the compounds **1** and **2** is that the EPR parameters in aqueous solution suggest a d_{z^2} ground state, whereas their geometry in the solid-state is very close to a regular octahedron. Indeed, the twist angles for **1**, **2**, as well as for $[V^{IV}(taci)_2](SO_4)_2 \cdot 12H_2O$,[15] $[V^{IV}(tdci)_2][V^{V}_4O_{12}] \cdot 14.5H_2O$,[15] and $[V^{IV}(tdci)_2H_{-1}]Cl_3 \cdot 15H_2O$[15] all fall in the range of 59.5−60°.[42] This could imply that a rearrangement of the structures takes place in water and that the angles in solution are lower than in the solid-state. To shed light on this problem, EPR spectra of the anion $[V(H_{-3}ino)_2]^{2-}$ were recorded by dissolving the solid complex **1** in a weakly coordinating solvent (DMF) or in a mixture of the non-coordinating solvents $CHCl_3$ and toluene (60:40 v/v). Analogous measurements were performed for the two cations $[V(taci)_2]^{4+}$ and $[V(tdci)_2]^{4+}$. The spectra of $[V(H_{-3}ino)_2]^{2-}$ are shown in Figure 9, whereas those of $[V(taci)_2]^{4+}$ and $[V(tdci)_2]^{4+}$ are reported in Figures S7 and S8 of the Supporting Information. EPR parameters are presented in Table 5. A better resolution in $CHCl_3$/toluene 60:40 v/v than in DMF is observed for all three complexes.

Examination of Figure 9 reveals that the spectra of $[V(H_{-3}ino)_2]^{2-}$ in DMF and in a mixture $CHCl_3$/toluene 60:40 v/v are comparable to that recorded in aqueous solution. A slight increase of the anisotropy parameter $|A_x - A_y|$ can be detected (Table 5). This means that the almost regular octahedral structure remained virtually unchanged in the three systems. An analogous trend is observed for $[V(taci)_2]^{4+}$ and $[V(tdci)_2]^{4+}$ (Table 5 and Figures S7 and S8, Supporting Information), with the complex formed by tdci reaching the maximum of anisotropy along the *x* and *y* directions in the organic solvents. For a complex with octahedral geometry, the observation of a d_{z^2} ground state is not expected. Obviously, the non-oxo vanadium(IV) complexes of ino and its derivatives do not follow the proposed behavior.[46] At the moment, the reason for this contradiction is not clear and must be further examined. It is possible that other effects, beside the distortion of the complexes, could contribute to determine the ground state of these complexes.

Conclusions and Outlook

Ino and its 1,3,5-trimethylated derivative tmci are able to form non-oxo vanadium(IV) complexes of composition $[V(H_{-3}L)_2]^{2-}$ (L = ino, tmci) by using three axial alkoxo groups for metal binding. The compound $[V(H_{-3}ino)_2]^{2-}$ has been thoroughly characterized in the solid-state and in aqueous solution. In analogy to taci and tdci,[15] the favorable metal binding properties of ino and tmci are based on the high degree of preorganization of the donor sets. However, in contrast to taci and tdci, $[V(H_{-3}ino)_2]^{2-}$ forms three distinct isomers in weakly basic aqueous solution with a bis-(ax−ax−ax), an (ax−ax−ax)−(ax−eq−ax), or a bis-(ax−eq−ax) structure. The non-observance of any (ax−eq−ax) isomers for the vanadium(IV)/taci and vanadium(IV)/tdci system obviously follows from the relatively low affinity of the very hard vanadium(IV) ion for nitrogen donors.

(46) Jezierski, A.; Raynor, J. B. *J. Chem. Soc. Dalton Trans.* **1981**, 1−7.
(47) Desideri, A.; Raynor, J. B.; Diamantis, A. A. *J. Chem. Soc. Dalton Trans.* **1978**, 423−426.
(48) Olk, R. M.; Dietzsch, W.; Kirmse, R.; Stach, J.; Hoyer, E.; Golic, L. *Inorg. Chim. Acta.* **1987**, *128*, 251−259.

Compared to taci and tdci, which can coordinate as neutral zwitterions with deprotonated oxygen donors and protonated nitrogens, the generation of three deprotonated oxygen donors in ino and tmci requires the action of an external base. As a consequence, formation of the anionic non-oxo species $[V(H_{-3}L)_2]^{2-}$ (L = ino, tmci) occurs at a higher pH as compared to the cationic $[VL_2]^{4+}$ complexes (L = taci, tdci). Because of the high number of coordinated alkoxo and non-coordinating hydroxy groups, $[V(H_{-3}ino)_2]^{2-}$ can serve as a versatile building block for supramolecular architectures. The interlinking of these building blocks can occur either by hydrogen bonding, in which the $[V(H_{-3}ino)_2]^{2-}$ unit can serve as a hydrogen donor or a hydrogen acceptor, or by binding additional cations. The two complexes **1** and **2** are illustrative examples for such molecular architectures.

In taci, tdci, ino, and tmci, the presence of non-hydrogen substituents in the 1, 3, and 5 positions helps to stabilize a rigid chair conformation of the cyclohexane ring, with the three axial oxygen donors forming an equilateral triangle that has an almost ideal orientation for a facial coordination of a metal center. In the solid-state, the corresponding bis-complexes all adopt approximate D_{3d} symmetry with a twist angle Φ close to 60°. There is good evidence that this structure is retained in solution. However, the EPR results indicate that these complexes have a d_{z^2} ground state that has been proposed to be characteristic of a structure with a significant distortion toward a trigonal prism (D_{3h}).[46−48] We propose that EPR theory in this field is incomplete and has to be revised.

In the light of insulin-enhancing effects of the vanadium compounds,[7−9] we plan to study the biological activity of such solid non-oxo vanadium(IV) complexes. They are relatively stable at the physiological pH and undergo conversion reactions to the $V^{IV}O$ di-hydroxo species only at higher pH values (see Figure 5). They could be of particular interest because ino and its derivatives are relatively nontoxic, and cell membranes have effective receptors for such polyalcohols. The investigation of taci, tdci, ino, and tmci complexes would allow us to study the effect of the overall charge of cationic and anionic species on the insulin-enhancing action and to compare their efficacy with respect to that of $V^{IV}O$ complexes. To the best of our knowledge, no study on the insulin-enhancing activity of non-oxo vanadium(IV) complexes has been reported in the literature.

Acknowledgment. We thank Anton Zaschka for the preparation of ino, Dr. Volker Huch for collecting X-ray diffraction data, and Dr. Holger Kohlmann for helpful discussions. Financial Support for B.K. from the E.U. Specific Targeted Research Project "Innovative tools for membrane protein structural proteomics (IMPS)" is gratefully acknowledged.

Supporting Information Available: Figures showing the kinetics of equilibration for the batch titration (Figure S1), X-band anisotropic EPR spectra of $[(VO)_2(ino)_2H_{-5}]^-$ (Figure S2), of $[V(H_{-3}ino)_2]^{2-}$ (Figure S3), of $[V(H_{-3}ino)_2]^{2-}$ as a function of the time (Figure S4), of $[V(H_{-3}tmci)_2]^{2-}$ as a function of pH (Figure S5), of $[V(H_{-3}tmci)_2]^{2-}$ (Figure S6), of $[V(taci)_2]^{4+}$ and $[V(tdci)_2]^{4+}$ in several solvents (Figures S7 and S8). Crystallographic data in CIF format for the reported structures. This material is available free of charge via the Internet at http://pubs.acs.org.

IC0618504